Functional and Structural Characterization of a Synthetic Peptide Representing the N-Terminal Domain of Prokaryotic Pyruvate Dehydrogenase†

Annechien F. Hengeveld,‡ Carlo P. M. van Mierlo, Henno W. van den Hooven,§ Antonie J. W. G. Visser, and Aart de Kok*

Laboratory of Biochemistry, Wageningen University, Dreijenlaan 3, 6703 HA Wageningen, The Netherlands

Received December 19, 2001

ABSTRACT: A synthetic peptide (Nterm-E1p) is used to characterize the structure and function of the N-terminal region (amino acid residues 4−45) of the pyruvate dehydrogenase component (E1p) from the pyruvate dehydrogenase multienzyme complex (PDHC) from *Azotobacter vinelandii*. Activity and binding studies established that Nterm-E1p specifically competes with E1p for binding to the dihydrolipoyl transacetylase component (E2p) of PDHC. Moreover, the experiments show that the N-terminal region of E1p forms an independent folding domain that functions as a binding domain. CD measurements, two-dimensional (2D) ^{1}H NMR analysis, and secondary structure prediction all indicate that Nterm-E1p has a high α-helical content. Here a structural model of the N-terminal domain is proposed. The peptide is present in two conformations, the population of which depends on the sample conditions. The conformations are designated "unfolded" at pH ≥6 and "folded" at pH <5. The 2D ^{1}H TOCSY spectrum of a mixture of folded and unfolded Nterm-E1p shows exchange cross-peaks that "link" the folded and unfolded state of Nterm-E1p. The rate of exchange between the two species is in the range of 0.5−5 s^{-1}. Sharp resonances in the NMR spectra of wild-type E1p demonstrate that this 200 kDa enzyme contains highly flexible regions. The observed dynamic character of E1p and of Nterm-E1p is likely required for the binding of the E1p dimer to the two different binding sites on E2p. Moreover, the flexibility might be essential in sustaining the allosteric properties of the enzyme bound in the complex.

The pyruvate dehydrogenase multienzyme complex (PDHC)[1] from Gram-negative bacteria consists of multiple copies of three different enzyme components: pyruvate dehydrogenase (E1p), dihydrolipoyl transacetylase (E2p), and lipoamide dehydrogenase (E3). The complex catalyzes the oxidative decarboxylation of pyruvate and the subsequent acetylation of coenzyme A to acetyl-CoA (for reviews, see refs *1*−*5*). The substrate specific, thiamin diphosphate-dependent E1p catalyzes the decarboxylation of pyruvate and subsequently the reductive acetylation of the lipoamide groups attached to E2p. The E2p component then transfers the acyl group to CoA. Finally, the reduced lipoyl group is re-oxidized by the FAD-dependent E3 component, which transfers the reduction equivalents to NAD^+.

E2p plays a central role in the complex, both catalytically and structurally. From the N-terminus to the C-terminus, it consists of two or three lipoyl domains, each carrying a lipoyllysine group, an E1/E3 binding domain, and a catalytic domain that also forms the structural core of the complex. Three-dimensional (3D) structures of the different domains of E2p have been determined either by X-ray crystallography (*6*−*10*) or by NMR spectroscopy (*11*−*16*).

The E1/E3 binding domain of E2p behaves like a Janus-face protein. E3 interacts solely with the N-terminal helix of the E1/E3 binding domain, while E1p interacts with the C-terminal part of the E1/E3 binding domain. The mode of binding of *Bacillus stearothermophilus* E3 to the binding domain was determined by X-ray crystallography (*17*). The binding site for E1p, unlike the binding site for E3, consists of two regions, one located on the E1/E3 binding domain of E2p and one on the catalytic domain of E2p (*18*). This was confirmed by the construction of *Azotobacter vinelandii*−*Escherichia coli* chimeric E2p (*19*). E1p only interacts strongly with a chimeric E2p when both the E1/E3 binding domain and the catalytic domain are of the same origin as E1p.

Recently, the three-dimensional structures of the heterotetrameric ($\alpha_2\beta_2$) branched-chain oxoacid dehydrogenase (E1b) from *Pseudomonas putida* and from humans were determined (*20*, *21*). No structural information is available though for

† This work was supported by the Netherlands Foundation for Chemical Research (CW) with financial aid from the Netherlands Organisation for Scientific Research (NWO).

* To whom correspondence should be addressed. Phone: +31 317 483866. Fax: +31 317 484101. E-mail: Aart.deKok@fad.bc.wau.nl, Carlo.vanMierlo@nmr.bc.wau.nl, and Ton.Visser@laser.bc.wau.nl.

‡ Present address: Leiden Amsterdam Center for Drug Research, Department of Pharmacochemistry, Vrije Universiteit Amsterdam, De Boelelaan 1083, 1081 KH Amsterdam, The Netherlands. Phone: +31 20 4447713. Fax: +31 20 4447755. E-mail: Hengveld@chem.vu.nl.

§ Present address: Akzo Nobel, Organon, RX 1110, P.O. Box 20, 5340 BH Oss, The Netherlands. Phone: +31 412 639422. Fax: +31 412 639444. E-mail: Henno.vandenHooven@Organon.com.

[1] Abbreviations: Cl_2Ind, 2,6-dichlorophenolindophenol; DSS, 2,2-dimethyl-2-silapentane-5-sulfonic acid; E1b, branched-chain α-keto acid decarboxylase (EC 1.2.1.25); E1p, pyruvate dehydrogenase (EC 1.2.4.1); E2p, dihydrolipoyl transacetylase (EC 2.3.1.12); E3, lipoamide dehydrogenase (EC 1.8.1.4); GuHCl, guanidinium hydrochloride; MP-8, microperoxidase 8; NOE, nuclear Overhauser effect; Nterm-E1p, peptide representing amino acids 4−45 of E1p from *A. vinelandii*; PDHC, pyruvate dehydrogenase multienzyme complex; TFA, trifluoroacetic acid; ThDP, thiamin diphosphate; TLCK, L-1-chloro-3-(4-tosylamido)-7-amino-2-heptanone-HCl; TMA, tetramethylammonium nitrate; TPPI, time-proportional phase incrementation.

10.1021/bi012172u CCC: $22.00
Published on Web 05/11/2002

the homodimeric (α_2) E1. However, recent studies (*22*) have provided insight into the mode of binding of homodimeric E1p to E2p. Limited proteolysis experiments with *A. vinelandii* E1p showed that its N-terminal region (amino acids 1−50) could easily be cleaved off. The remaining fragment is still active, but unable to bind to E2p. This suggests that the N-terminal region is involved in the binding to E2p, but not in catalysis. The role of the N-terminal sequence of *A. vinelandii* E1p in the binding to E2p was confirmed by the construction of a series of N-terminal deletion mutants (*23*). Construction of a heterodimeric E1p, containing only one N-terminal region, demonstrated that not one but both N-termini of the homodimer are necessary for good binding.

From the previous studies, it is not evident whether the N-terminal region of E1p forms an independent folding domain and, if so, how this domain functions. To attempt to answer these questions, a synthetic peptide called Nterm-E1p is used in both functional and detailed spectroscopic studies. The design of the peptide is based on the following considerations. First, deletion experiments show that the structural core of E1p starts from amino acid 49 (*23*). Second, amino acids R37, E40, and R44 are all highly sensitive to proteases, indicating a more flexible or extended region and thus the end of the N-terminal domain (*22*). Third, deletion experiments show that amino acid residues 1−8 are not required or necessary for the functional integrity of the binding domain (*23*). Fourth, due to the decrease in the accuracy of the peptide synthesis upon the increase in peptide size, the size of the peptide had to be minimized. Consequently, we decided to construct a peptide starting at Met4 and ending at Thr45.

EXPERIMENTAL PROCEDURES

Peptide Synthesis

A peptide consisting of 42 amino acid residues (designated Nterm-E1p) (MQDLDPIETQEWLDSLESVLDHEGEERAHYLLTRMGELATRT) that mimics the N-terminal region of E1p was synthesized by Genosys Biotechnologies. The peptide was supplied lyophilized and purified (84%) by reversed phase high-performance liquid chromatography (HPLC) using an acetonitrile/water solvent gradient containing 0.1% trifluoroacetic acid (TFA). The peptide was further purified to 98% by HPLC using the same solvents. The purity of the sample was judged by analysis of the integrals of the elution peaks.

Enzyme Isolation

E. coli strain TG2, a *recA*$^-$ version of TG1 [Δ(*lac*$^-$*proAB*), *thi*, *supE*, *Res*$^-$ *Mod*$^-$ (*k*), *F*′ (*traD36 proA*$^+$*B*$^+$, *lacI*^{q} *lacZ* ΔM15)] (*24*) harboring the recombinant plasmid pAFH001, expressing wild-type E1p was grown and purified as described in ref *22*. *A. vinelandii* wild-type E2p and E3 were expressed and purified from *E. coli* TG2 cells as described in refs *25* and *26*. *A. vinelandii* E3-Y16F was expressed and purified as described in ref *27*.

Activity Assays

The oxidative decarboxylation of pyruvate by E1p was measured at 600 nm using 2,6-dichlorophenolindophenol (Cl_2Ind) ($\epsilon = 21.7 \times 10^3\ M^{-1}\ cm^{-1}$) as an artificial electron acceptor (*28*). The E2p component was assayed as described in ref *29*. The E3 and E3-Y16F component were assayed as described in ref *30*. The overall PDHC activity was reconstituted by incubating E2p with E1p and E3 or E3-Y16F and was measured spectrophotometrically at 340 nm as described in ref *31*.

Binding Studies

The binding of Nterm-E1p to E2p was analyzed by analytical size-exclusion chromatography using a Superose 6 column (Pharmacia Biotech) as described in ref *22*. The collected fractions were analyzed by SDS−PAGE (*32*). The E2p concentration was 8.3 μM; the Nterm-E1p concentration was 40.6 μM.

Protein concentrations were estimated using the microbiuret method (*33*). Bovine serum albumin was used as a standard.

Limited Proteolysis and MALDI-TOF MS

Truncated *A. vinelandii* E1p for NMR spectroscopy was obtained by limited proteolysis of E1p by endoproteinase GluC as described in ref *23*. A 1 mg/mL concentration of E1p was used, and the reaction was stopped by addition of TLCK (final concentration of 260 μM). After proteolysis, the small fragments and the protease were removed from the sample by ultrafiltration, using a 100 kDa cutoff filter. This step was repeated three times. The sample was concentrated to the original starting volume of the undigested E1p NMR sample, resulting in a concentration of approximately 0.5 mM of digested E1p.

For MALDI-TOF MS, truncated *A. vinelandii* E1p was obtained by limited proteolysis of the enzyme by endoproteinase GluC as described in ref *23*. The small fragments were separated from the large (core) fragment on a Superdex peptide column. The collected fractions were freeze-dried and subsequently dissolved in 20−100 μL of water. The remaining salt was removed by use of cation exchange chromatography (Biorad AG50W-X8 column). Finally, the samples, which were changed by hydrophobic interaction chromatography (Millex-FH, Millipore Corp.) into 50% AcNi and 0.1% TFA/H_2O, were analyzed by MALDI-TOF MS on an applied Biosystems voyager DE RP using *x*-cyano 4-hydroxycynamic acid as a matrix solution. TFA was used to decrease the pH of the samples. Microperoxidase (MP-8) (*34*) was used for calibration.

Spectroscopic Measurements

Circular Dichroism Spectroscopy. CD spectra were recorded at 20 °C on a Jasco spectropolarimeter (model J-715). Spectra were recorded in cuvettes with a 0.1 cm path length. The peptide concentration was 10.1 μM (50 μg/mL) in 10 mM potassium phosphate (pH 4.8). The pH was adjusted by addition of aliquots of 250 mM NaOH or of 250 mM HCl to values ranging from pH 3 to 7. The ionic strength was increased by the addition of aliquots of 3 M KCl.

Fluorescence Spectroscopy. The fluorescence emission spectra were measured on a Fluorolog 3 (SPEX) fluorimeter at several temperatures using an excitation wavelength of 280 or 295 nm, with 1 nm slits. The sample conditions were identical to those described for the CD measurements. Spectra were recorded in 1 mL fluorescence cuvettes with a 1 cm path length.

Time-Resolved Fluorescence Spectroscopy. Time-resolved fluorescence measurements were carried out using mode-

locked continuous wave lasers and time-correlated counting as a detection technique. A mode-locked CW yttrium lithium fluoride (YFL) laser was used for the synchronous pumping of a cavity-dumped rhodamine 6G dye laser. The sample volumes were 1 mL with a light path of 1 cm. Fluorescence was detected at an angle of 90° with respect to the excitation light beam. An interference filter (Schott, 348.8 nm) was used for detection. Measurements consisted of repeated sequences of measuring during 10 s of parallel and 10 s of perpendicular polarized emission. Background emission of the buffer solution was measured and used for background subtraction. The fast and single-exponential fluorescence decay of *p*-terphenyl in a 50/50 cyclohexane/CCl_4 mixture was measured to obtain a dynamic instrumental response. Data analysis was performed using a home-built computer program (*35*). The peptide concentration was 10.1 or 20.2 μM in 10 mM potassium phosphate (pH 4.8). The pH was adjusted by the addition of aliquots of 250 mM NaOH or 250 mM HCl. The E2p concentration was 3.5 or 7.0 μM.

NMR Spectroscopy. Samples of the peptide Nterm-E1p contained 4.05 mM protein in a 90% H_2O/10% ^2H_2O mixture [one-dimensional (1D) NMR measurements] or 8.1 mM protein in a 90% H_2O/10% ^2H_2O mixture [two-dimensional (2D) NMR measurements]. The E1p samples contained 0.5 mM protein in a 90% H_2O/10% ^2H_2O mixture. The pH was adjusted by the addition of a small amount of a solution of 250 mM NaOH or 250 mM HCl. ThDP was added to the E1p and to the truncated E1p sample to a concentration where the NMR signals originating from free ThDP were just visible in the recorded NMR spectra. Truncated E1p was obtained by limited proteolysis of E1p by endoproteinase GluC as described above. The E1p NMR sample was diluted to a concentration of 1 mg/mL. NOESY (τ_m = 50 ms) (*36*, *37*) and TOCSY (τ_m = 50 ms) (*38*) spectra were acquired on a Bruker AMX500 spectrometer. The used carrier frequency coincided with the water resonance. The sample temperature was maintained at 284 or 298 K as calibrated with tetramethylammonium nitrate (TMA). The NOESY spectra were acquired with presaturation during the relaxation delay and mixing time. The TOCSY spectra were acquired using homonuclear Hartman−Hahn transfer using the clean-MLEV17 sequence for mixing, using two power levels for excitation and spin lock (*39*, *40*). Time-proportional phase incrementation (TPPI) (*41*) was used in all experiments. The TOCSY experiments were recorded with 120 t_1 experiments and 2048 data points. The TOCSY experiment of E1p was recorded with 64 t_1 experiments and 2048 data points. The NOESY experiments were recorded with 176 t_1 experiments and 2048 data points. The spectral width was 8406 Hz. The chemical shift is reported relative to an external standard [2,2-dimethyl-2-silapentane-5-sulfonic acid (DSS)]. The obtained data were processed using XWINNMR software (Bruker). The data were digitally filtered using a sine-bell shifted by 45° in the t_2 dimension and a squared cosine-bell in the t_1 dimension. After double Fourier transformation and interactive phase correction, a baseline correction with a polynomial with an order of 5 was performed for all spectra. The 2D spectra are presented as contour plots with 14 levels increasing by a factor of 1.3.

A 1D version of the three-pulse NOESY sequence and phase cycle was used to collect the 1D NMR data. No window functions were applied to the 1D NMR data, and no zero filling was applied.

RESULTS

Functionality of the Peptide Representing the N-Terminal Region of E1p

To establish the function of the N-terminal region of E1p from *A. vinelandii*, a synthetic peptide representing amino acid residues 4−45 of E1p is used. Initially, attempts were made to obtain the N-terminal region by limited proteolysis of E1p using endoproteinase GluC. The small fragments obtained after partial proteolyses were analyzed by MALDI-TOF MS. A wide range of fragment sizes was found ranging from 392 to 1507 Da. On the basis of the sequence, fragments ranging from 285 to 4759 Da (3−40 amino acids) were predicted. The expected molecular mass of the entire N-terminal domain is ∼4700 Da, indicating that the N-terminal region itself is sensitive to the protease and that it is digested into small (3−13 amino acids) fragments.

Since we were not able to isolate the N-terminal region itself by the above-described method, the synthetic peptide "Nterm-E1p" was used in our studies. For reasons described in the introductory section, a region of the N-terminus of E1p was chosen that starts at amino acid 4 and ends at amino acid 45. To determine whether this peptide forms a functional binding domain, several functional studies were performed.

First, complex activity was measured. E2p was incubated with different concentrations of Nterm-E1p; subsequently, E1p and E3 were added, and finally, complex activity was measured (Figure 1). To establish whether Nterm-E1p competes for binding to E2p with E1p, with E3, or with both, the mutant E3-Y16F (*27*) was used instead of wild-type E3. This dimer interface mutant is impaired in its dimerization (E3−E3) and virtually inactive. Upon binding to E2p, however, it forms a stable and active dimer. This enables us to distinguish between the bound and unbound form of E3. Figure 1 shows the results of a titration of E2p with Nterm-E1p and the subsequent recombination with E1p and E3-Y16F. The results show that Nterm-E1p inhibits complex activity, whereas it has no influence on the activity of E3-Y16F. Maximum inhibition is ∼45% at a 20:1 Nterm-E1p:E2p ratio. This partial inhibition can be caused by several factors. First of all, it is possible that the apparent maximum inhibition is not a real plateau but a very shallow increasing slope that will reach 100% inhibition at infinite peptide concentration. On the other hand, it could also be that the peptide can only interact with one of the two E1p binding sites on E2p and therefore can only partially inhibit the binding of E1p to E2p. The activities of the different components of the complex in the presence of a 15-fold excess of Nterm-E1p were measured, and no significant effect was found. Consequently, the inhibitory effect on complex activity must be due to competition of Nterm-E1p with either E1p, E3, or both for binding to E2p. As no effect of Nterm-E1p on the E3-Y16F activity was measured (Figure 1), Nterm-E1p must be competing with E1p for specific interactions with one or both of the E1p binding sites on E2p. It is very difficult to accurately calculate a binding constant for Nterm-E1p. The measured reaction is very complex; it involves three enzyme components and an inhibitor. Moreover, E1p and E3 influence each other's binding to E2p (*42*).

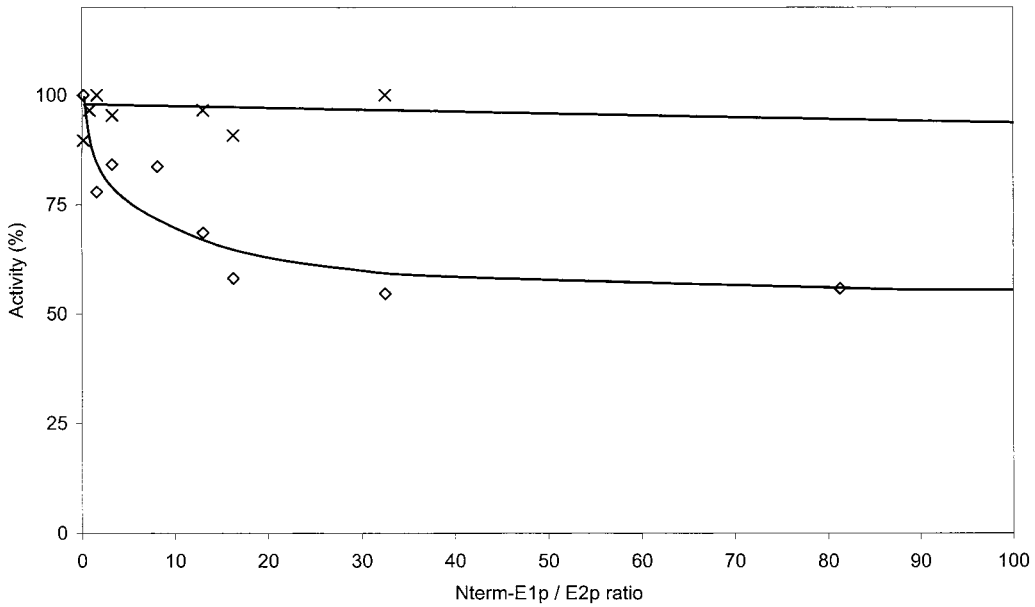

FIGURE 1: Reconstitution of *A. vinelandii* PDHC in the presence of a varying concentration of Nterm-E1p. E2p (1.6 μM) was incubated with varying concentrations of Nterm-E1p. Subsequently, it was recombined with E1p (1.6 μM) and mutant E3-Y16F (1.0 μM) (*26*), and finally, after incubation for 15 min, complex activity (◇) and E3 activity (×) were measured.

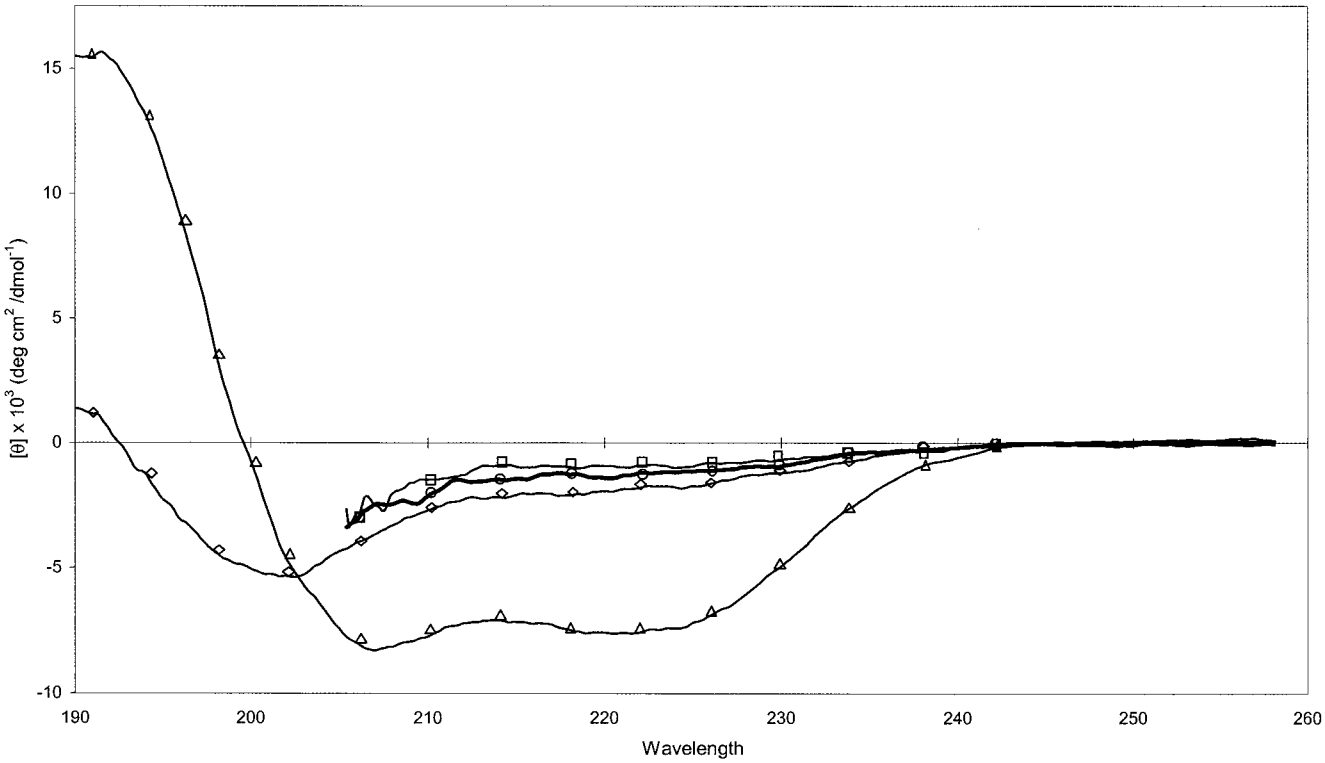

FIGURE 2: Far-UV CD spectrum of Nterm-E1p at varying pH values and in the presence of different concentrations of GuHCl. The samples were prepared as described in Experimental Procedures: Nterm-E1p at pH 4.8 (△), Nterm-E1p at pH 6.8 (◇), Nterm-E1p at pH 6.8 with 0.6 M GuHCl (○), and Nterm-E1p at pH 6.8 with 1.2 M GuHCl (□).

Second, the binding of Nterm-E1p to E2p was monitored by analytical gel filtration (data not shown); free E2p mainly elutes in a "24-mer" peak, but upon addition (and binding) of E1p or E3, it dissociates into trimers. An analytical gel filtration column can separate these fractions very well (*18*, *21*). When E2p is preincubated with an excess amount of Nterm-E1p (1:5 ratio), one extra elution peak appears at an elution volume expected for Nterm-E1p. Whereas the integral of the E2p elution peak increases, its elution volume does not change compared to the elution volume of the free E2p sample. This demonstrates that although Nterm-E1p binds to E2p it does not (unlike wild-type E1p) influence the trimer−trimer interactions of E2p.

Nterm-E1p Has a pH-Dependent Conformation

CD Measurements. The conformational behavior of Nterm-E1p was investigated using CD, fluorescence, and NMR spectroscopy. The CD results are shown in Figure 2. At pH 4.8, a spectrum with two minima at 208 and 222 nm and a crossover point at 200 nm is observed, which is characteristic

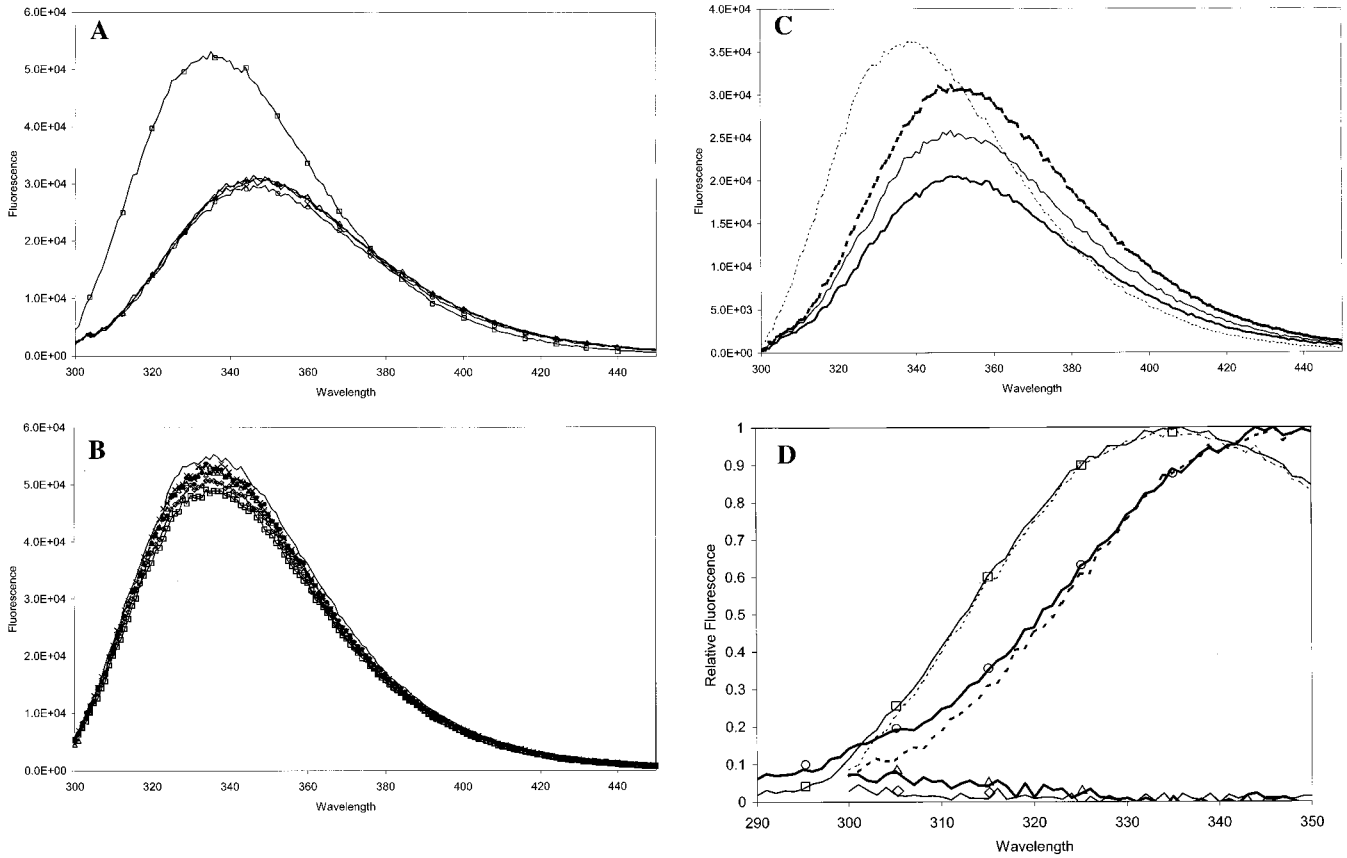

FIGURE 3: Fluorescence spectra obtained with excitation at 295 nm of Nterm-E1p at varying pH values (A), at varying ionic strengths (B), and in the presence of various concentrations of the denaturant GuHCl (C). Normalized fluorescence spectra obtained with excitation at 280 nm of Nterm-E1p at pH 4.8 and 6.8 are shown in panel D. Difference spectra were obtained by normalizing the fluorescence spectra and subtracting the spectrum obtained with excitation at 295 nm from the spectrum obtained with excitation at 280 nm. (A) Nterm-E1p at pH 4.8 (□), pH 5.5 (○), pH 6.2 (△), and pH 6.8 (◇). (B) Nterm-E1p at pH 4.8 (△), Nterm-E1p at pH 5 with 50 mM KCl (□), Nterm-E1p at pH 5 with 100 mM KCl (◇), Nterm-E1p at pH 5 with 150 mM KCl (×), Nterm-E1p at pH 5.2 with 250 mM KCl (●), and Nterm-E1p at pH 5.2 with 400 mM KCl (—). (C) Nterm-E1p at pH 4.8 (thin dotted line), Nterm-E1p at pH 6.8 thick dotted line), Nterm-E1p at pH 6.8 with 0.6 M GuHCl (thin line), and Nterm-E1p at pH 6.8 with 1.2 M GuHCl (thick line). (D) Nterm-E1p at pH 4.8 with excitation at 280 nm (□), Nterm-E1p at pH 4.8 with excitation at 295 nm (thin dotted line), Nterm-E1p at pH 6.8 with excitation at 280 nm (○), Nterm-E1p at pH 6.8 with excitation at 295 nm (thick dotted line), the difference spectrum of Nterm-E1p at pH 4.8 (◇), and the difference spectrum of Nterm-E1p at pH 6.8 (△).

Table 1: Secondary Structure Content of Nterm-E1p at Different pH Values As Calculated from CD Measurements by the Program CONTIN (*41*)[a]

	α-helix (%)	β-sheet (%)	β-turn (%)	unfolded (%)	unknown (%)
pH 4.8	67	0	14	19	–
pH 6.8	12	24	10	54	–
prediction	73	0	17	–	10

[a] The predicted secondary structure content of the peptide as determined using the neural network algorithms from the European Molecular Biology Laboratory (EMBL) (*48*, *49*) is also shown. The samples were prepared as described in Experimental Procedures.

of a highly α-helical conformation. At pH 6.8, the CD spectrum exhibits only a minimum at 203 nm and the crossover point is shifted to 193 nm, which is more typical for an unfolded protein. To evaluate the secondary structure of Nterm-E1p, the program CONTIN was used (*43*) (Table 1). Indeed, at pH 4.8, the peptide is mostly α-helical (68%), while at pH 6.8, it is mostly unordered (54%). For brevity, from here on, the conformation of the peptide at pH 4.8 is termed "folded" and the conformation of the peptide at pH 6.8 is termed "unfolded". We are aware that this does not fully describe the conformation of the peptide under these conditions and have conducted more detailed studies using NMR and fluorescence spectroscopy to determine the conformation of Nterm-E1p under various conditions in more detail (see below).

Fluorescence Measurements. Nterm-E1p contains a single tryptophan, and therefore, fluorescence spectroscopy is a very suitable technique for studying the microenvironment of this residue. All experiments were recorded with excitation at 295 nm, where only tryptophan absorbs light. At pH 4.8, the tryptophan has a fluorescence maximum at 335 nm (Figure 3), while between pH 5.5 and 6.8, the maximum is at 350 nm. The emission maximum at 350 nm is typical for a tryptophan in a polar environment (with few protein contacts). The blue-shifted maximum at 335 nm and pH 4.8 results from a less polar environment, a tryptophan buried in a protein (i.e., in a folded structure). In addition, the fluorescence of the peptide at pH 6.8 is quenched by 40% compared to the fluorescence at pH 4.8, which is likely caused by the exposure of the tryptophan to the solvent, as a tryptophan's emission pattern is highly sensitive to the polarity of the solution. Thus, this local structure is in agreement with the CD observations that the peptide can exist in two conformations: folded and unfolded.

Table 2: Fluorescence Decay and Fluorescence Anisotropy Parameters of Nterm-E1p at pH 4.8 and pH 7.0 (duplicates)[a]

	fluorescence decay		fluorescence anisotropy				
	χ^2 [b]	τ [c]	χ^2	ϕ_1 [d] (ns) ([CI][e])	β_1 [f]	ϕ_2 (ns) ([CI])	β_2
pH 4.8	1.05	2.05	1.05	0.28 (0.14−0.52)	0.11 (0.073−0.14)	2.05 (1.62−2.85)	0.13 (0.094−0.17)
pH 4.8	1.08	2.08	1.05	0.31 (0.17−0.49)	0.12 (0.09−0.15)	2.32 (1.85−3.20)	0.12 (0.088−0.15)
pH 7.0	1.02	1.97	1.07	0.19 (0.032−ND[g])	0.066 (0.025−ND[g])	1.32 (1.10−1.92)	0.17 (0.087−0.20)
pH 7.0	0.99	2.00	1.03	0.18 (0.051−ND[g])	0.071 (0.033−0.12)	1.31 (1.11−1.75)	0.17 (0.11−0.20)

[a] Samples were prepared as described in Experimental Procedures. [b] Quality of fit criterion. [c] Average fluorescence lifetime. [d] Rotational correlation times. [e] The 67% confidence interval. [f] Relative contribution of ϕ to the total anisotropy. [g] Not defined.

Besides steady state fluorescence, time-dependent fluorescence decay and fluorescence anisotropy of the peptide at 348.8 nm were measured using time-resolved fluorescence measurements (Table 2). The fluorescence decay was in both cases (pH 4.8 and 7.0) best fitted using a four-component exponential decay. In the time-resolved fluorescence measurements, the average fluorescence lifetime of the peptide at pH 7.0 is slightly shorter than at pH 4.8 (Table 2), which is in agreement with the decreased fluorescence intensity in the steady-state measurements (Figure 3). A fluorescence lifetime of the tryptophan close to 2 ns was found for the peptide at both pH 4.8 and 7.0, indicating quenching of the tryptophan fluorescence under both conditions (the average lifetime of a tryptophan is ∼3 ns). This quenching can be caused by a nearby tyrosine, glutamine, glutamic acid, aspartic acid, or histidine (*44*, *45*).

The anisotropy decays of the peptide at pH 4.8 and 7.0 contain two components (Table 2): a short sub-nanosecond component and a component of 1−2 ns. The short component probably originates from the internal flexibility of the tryptophan. The smaller contribution of this component to the total fluorescence anisotropy at pH 7.0 compared to the contribution of the sub-nanosecond component at pH 4.8 probably results from a smaller amplitude of the movement of the tryptophan in the pH 7.0 sample. The second anisotropy component of the peptide at pH 4.8 correlates excellently with the expected rotational correlation time of a globular protein of 4.9 kDa (1.9 ns) (*46*). The shorter rotational correlation time (1.3 ns) of the peptide at pH 7.0 supports a changed, less compact, conformation under these conditions, i.e., the peptide being unfolded.

NMR Measurements. 1D ^{1}H NMR spectra of Nterm-E1p were recorded at pH values ranging from pH 5.0 to 6.5 (Figure 4). Due to the overlap of most of the NMR resonances, assignment of the resonances to their corresponding protons is not possible based on these 1D NMR spectra. An exception to the latter forms the resonance with a chemical shift of 10.12 ppm (in the spectrum recorded at pH 6.5). This resonance is assigned to the aromatic side chain NH of the single tryptophan in Nterm-E1p (*47*). At low pH, two resonances instead of one are found in the low-field region of the NMR spectrum. The new resonance emerges at a chemical shift of 10.43 ppm, and also originates from the aromatic side chain NH of the tryptophan residue (see following sections). The resonance at 10.43 ppm gives rise to many NOE cross-peaks in the 2D NOESY NMR spectrum (Figure 5), whereas the resonance at 10.12 ppm does not. Consequently, the resonance at 10.43 ppm corresponds to the aromatic NH of a tryptophan in a folded environment. The tryptophan aromatic NH resonance at 10.12 ppm has virtually no NOE contacts with the remainder of the peptide, and its chemical shift is typical for that of an exposed tryptophan, i.e., a tryptophan in an unfolded protein.

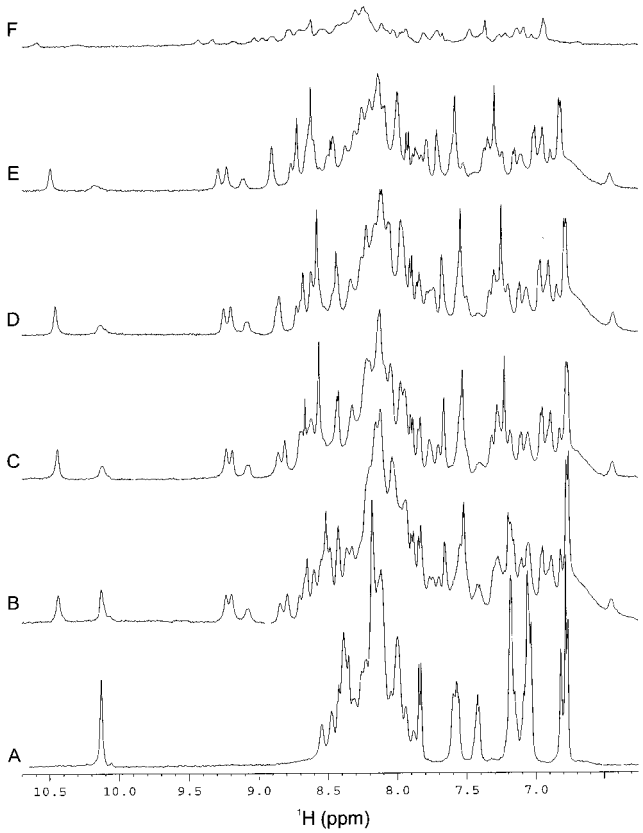

FIGURE 4: 500 MHz 1D ^{1}H NMR spectra of Nterm-E1p in a 90% H_2O/10% ^2H_2O mixture recorded at various pH values and various ionic strengths, at a temperature of 298 K. The samples were prepared as described in Experimental Procedures: (A) Nterm-E1p at pH 6.5, (B) Nterm-E1p at pH 5.8, (C) Nterm-E1p at pH 5.0, (D) Nterm-E1p at pH 5.0 with 138 mM KCl, (E) Nterm-E1p at pH 5.3 with 415 mM KCl, and (F) Nterm-E1p at pH 5.5 with 1 M KCl.

Equilibrium between the Folded and Unfolded Conformation of Nterm-E1p

The experiments described above show that the conformation of Nterm-E1p is pH-dependent. At pH 6.5, it seems to be largely unfolded, while at pH 5.0, a mixture of folded and unfolded peptides exists. Addition of a denaturant (GuHCl) at pH 6.8 results in a small reduction of the magnitude of the far-UV signal (Figure 2), suggesting some slight further unfolding of Nterm-E1p, but has no influence on the tryptophan fluorescence maximum (data not shown), showing that the peptide is largely unfolded under these conditions.

To test the influence of a change in the sample condition on the equilibrium between the folded and unfolded peptide,

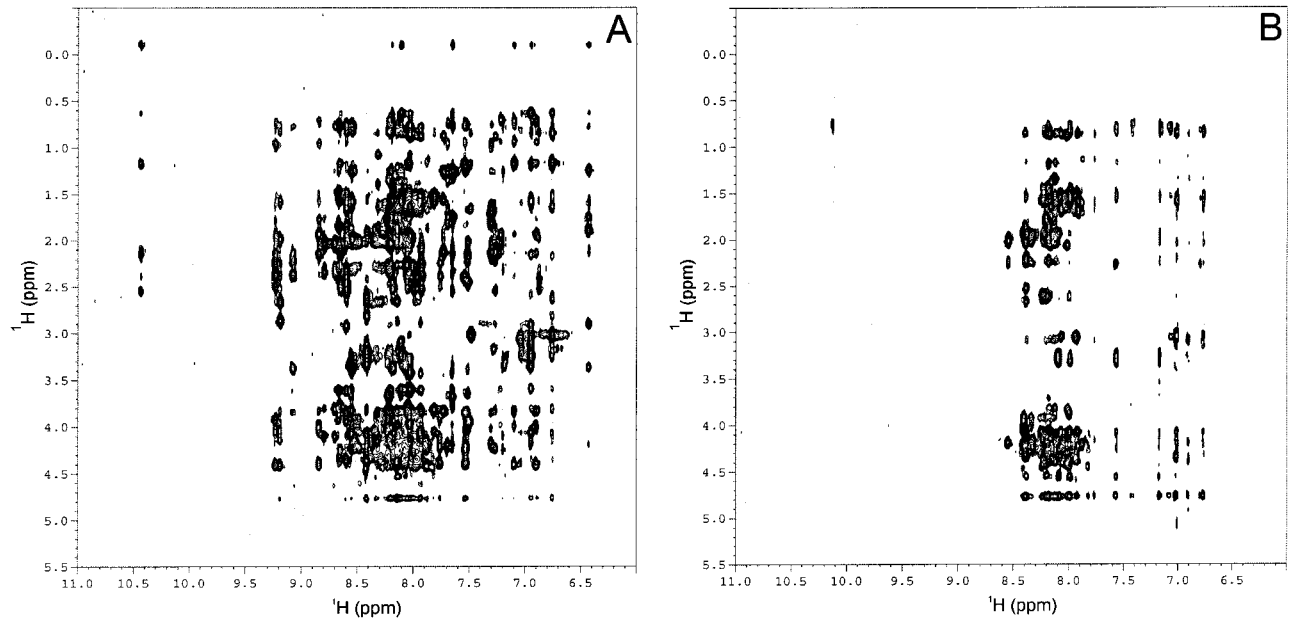

FIGURE 5: 500 MHz 2D ^{1}H NOESY spectra of Nterm-E1p in a 90% H_2O/10% ^2H_2O mixture recorded at pH 5.0 and 6.5 at a temperature of 298 K. The mixing time was 50 ms. (A) Fingerprint region of the NOESY spectrum of Nterm-E1p at pH 5.0. (B) Fingerprint region of the NOESY spectrum of Nterm-E1p at pH 6.5.

Table 3: Ratios of the Integrals of the Tryptophan Resonances at 10.43 and 10.12 ppm as a Function of pH and Ionic Strengths[a]

pH	[KCl] (mM)	10.43 ppm:10.12 ppm ratio
6.5	0	0:1
5.8	0	0.82:1
5.0	0	1.49:1
5.0	138	1.67:1
5.3	415	1.85:1
5.5	1000	1.20:1

[a] The tryptophan resonance at 10.43 ppm represents the folded state of Nterm-E1p, whereas the tryptophan resonance at 10.12 ppm represents the unfolded state of the peptide. The samples were prepared as described in Experimental Procedures.

1D ^{1}H NMR spectra were recorded at different ionic strengths (Figure 4). Additionally, fluorescence spectra were recorded at different ionic strengths (Figure 3), at different temperatures, and in the presence of different concentrations of GuHCl (Figure 3). Finally, CD spectra were recorded in the presence of different concentrations of GuHCl (Figure 2).

Table 3 shows the ratios of the integrals of the tryptophan resonances at 10.43 and 10.12 ppm at different pH values and at different ionic strengths. From Figure 4 and Table 3, it is clear that at pH 6.5 the folding equilibrium is completely shifted toward the unfolded state of the peptide. Under these conditions, only one resonance is observed for a tryptophan aromatic NH proton and the ^{1}H NMR spectrum has limited chemical shift dispersion, typical for that of a largely unfolded protein. The other sample conditions that were tested always resulted in a mixture of folded and unfolded Nterm-E1p. The folding equilibrium is shifted toward the folded state when the pH is lowered, but this effect is limited by the solubility of the peptide. At pH 3.5−4.3, the peptide precipitates due to protonation of the carboxyl groups of the peptide ($pK_a \sim 4$). For this reason, the lowest pH value used in our experiments was pH 4.8. Increasing the ionic strength of the solution by the addition of KCl results in a shift in the folding equilibrium toward the folded state; however, under these latter circumstances, significant line broadening of the NMR resonances is observed.

2D NMR: Analysis of the Secondary Structure of Nterm-E1p

To obtain more detailed information about the conformation of Nterm-E1p in the folded (pH 5.0) and unfolded (pH 6.5) states, 2D ^{1}H TOCSY and 2D ^{1}H NOESY NMR spectra were recorded (Figures 5 and 6). No attempt was made to obtain a complete sequential resonance assignment of the proton resonances of Nterm-E1p at pH 5 as the 2D NMR spectra are very complex. Two species are populated to a significant extent at pH 5; considerable resonance overlap is observed, and several signals are broadened due to exchange phenomena. In addition, as the synthetic peptide is not isotopically enriched, heteronuclear multidimensional NMR spectroscopy could not be employed to our benefit. For these reasons, only the main features of the 2D ^{1}H NMR spectra are discussed below.

Figure 6 shows the fingerprint and the NH cross-peak region of a TOCSY spectrum at pH 5 (Figure 6A,C) and at pH 6.5 (Figure 6B,D). The 2D ^{1}H TOCSY spectrum recorded at pH 6.5 is typical for a random coil protein, as it has limited backbone amide proton resonance dispersion (between 7.8 and 8.6 ppm). The 2D NMR spectrum of Nterm-E1p at pH 5, where a mixture of the folded and unfolded peptide exists, shows much more NH resonances and cross-peaks than the 2D NMR spectrum of Nterm-E1p at pH 6.5. The extra resonances that are observed fall outside the chemical shift ranges expected for an unfolded peptide. Approximately 10−15 d_{NN} NOEs are observed for the folded species. This is consistent with the CD results (Table 1) that indicate a significant α-helicity of the folded state.

Most of the NH resonances and cross-peaks in the TOCSY spectrum of unfolded Nterm-E1p are also present in the TOCSY spectrum acquired at pH 5. However, some of these resonances could not be observed in the TOCSY spectrum of the mixture of folded and unfolded Nterm-E1p. This can

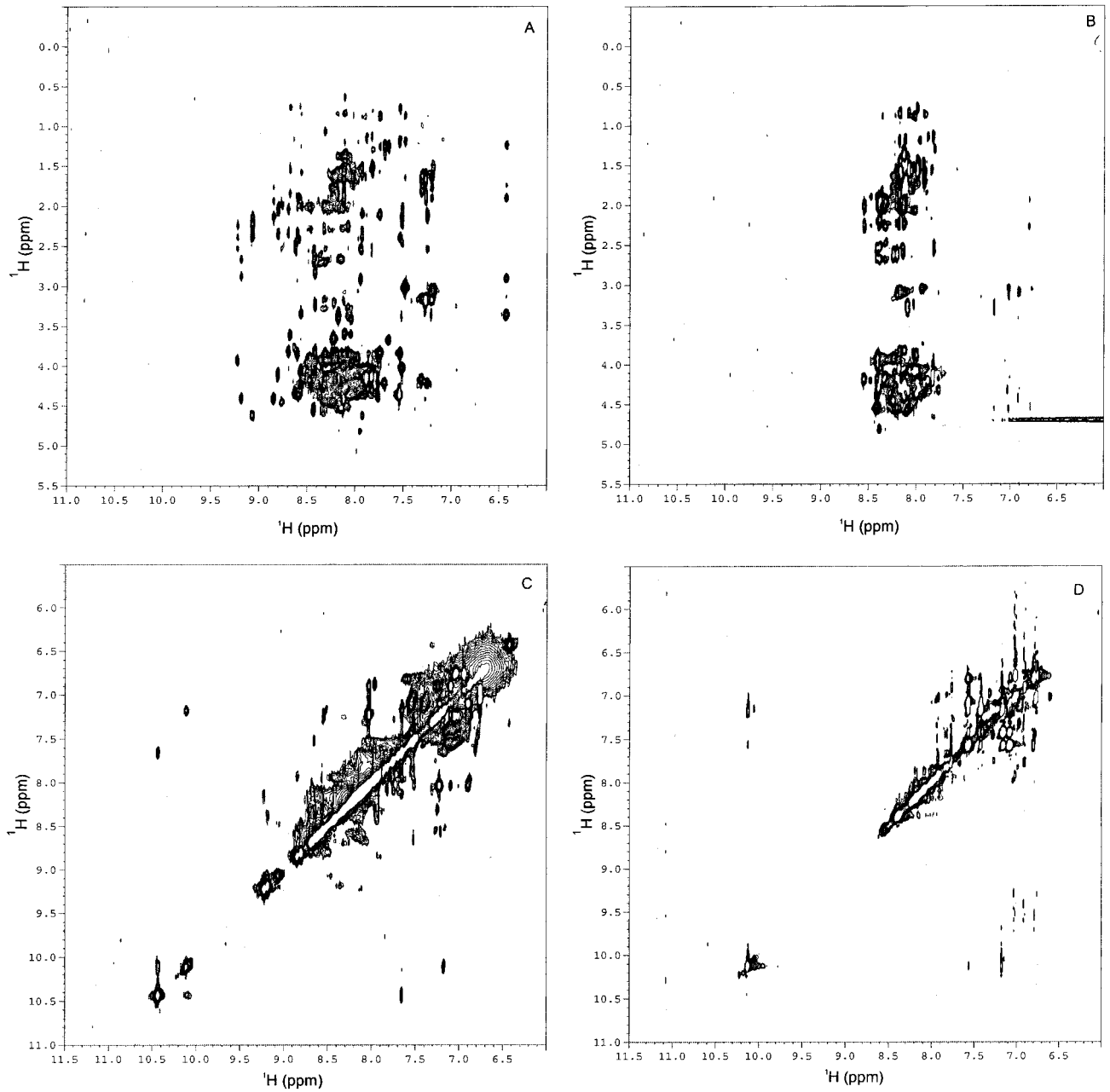

FIGURE 6: 500 MHz 2D ^{1}H TOCSY spectra of Nterm-E1p in a 90% H_2O/10% ^2H_2O mixture recorded at pH 5.0 and 6.5 at a temperature of 298 K. The mixing time was 50 ms. (A) Fingerprint region of the TOCSY spectrum of Nterm-E1p at pH 5.0. (B) Fingerprint region of the TOCSY spectrum of Nterm-E1p at pH 6.5. (C) NH cross-peak region of the TOCSY spectrum of Nterm-E1p at pH 5.0. (D) NH cross-peak region of the TOCSY spectrum of Nterm-E1p at pH 6.5.

be due to several reasons. First, the intensities of the cross-peaks of the peptide in the unfolded state are reduced in the TOCSY spectrum of the mixture of both folding states as only about half of the molecules are unfolded. Second, some signals in the 2D ^{1}H NMR spectra are severely broadened (compare panels A and B of Figure 6) as a result of exchange at an intermediate exchange rate on the chemical shift time scale, presumably between partially folded and fully unfolded molecules. Third, the pH change can cause the shift of several cross-peaks.

Rate of Exchange between Folded and Unfolded Nterm-E1p

Thus far, the peptide's function and conformation and the conditions that influence the equilibrium between the two conformations of the peptide were described. Here we focus on an interesting phenomenon displayed by the 2D ^{1}H TOCSY spectrum recorded at pH 5.0 and 298 K. This spectrum not only shows the two aromatic side chain NH resonances of the tryptophan in its folded and unfolded state but also shows a cross-peak that "links" these two resonances. Several similar cross-peaks are observed in the low-field region of the TOCSY spectrum (Figure 6C). These cross-peaks must be due to chemical exchange that is fast on the NMR T_1 time scale, but not on the chemical shift time scale ($\Delta\delta > k_{exch} > T_1^{-1}$). For the majority of these exchange cross-peaks, one of the frequencies could be assigned to the folded state of Nterm-E1p and the other frequency component resulted from the corresponding amide of unfolded Nterm-E1p. The exchange cross-peaks disappear once the folded state of Nterm-E1p is fully populated. Similar

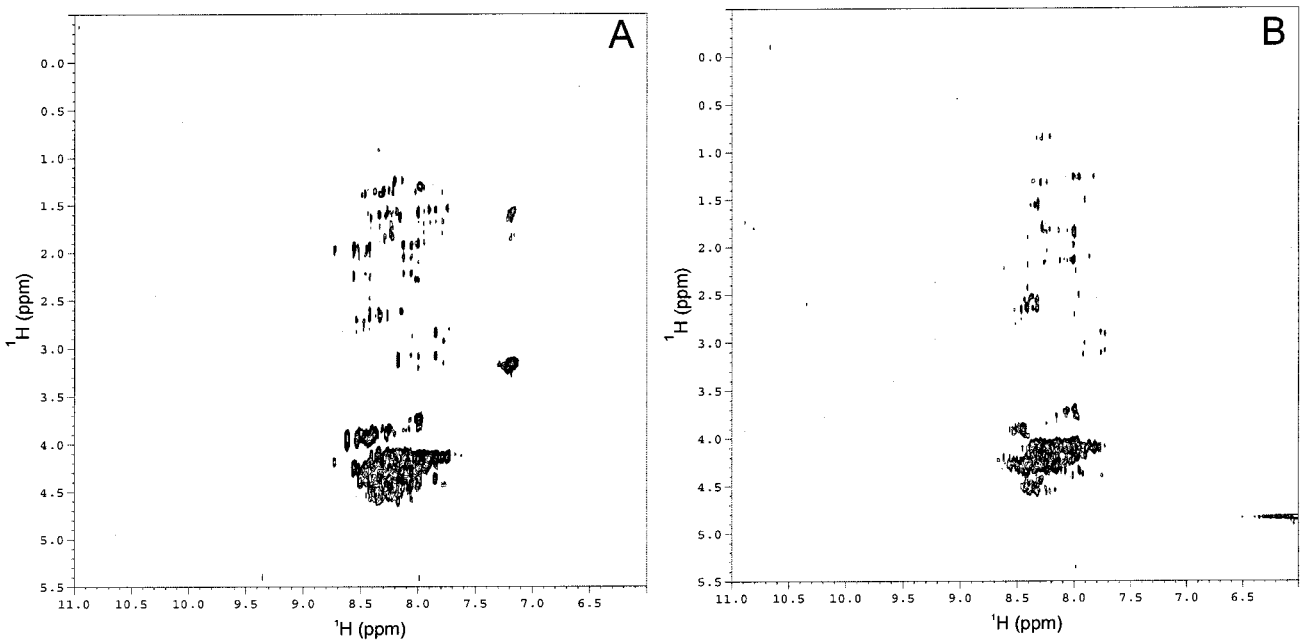

FIGURE 7: 500 MHz 2D ^{1}H TOCSY spectra of E1p and truncated E1p in a 90% H_2O/10% ^2H_2O mixture recorded at pH 6.5 at a temperature of 298 K. The mixing time was 50 ms. (A) Fingerprint region of the TOCSY spectrum of E1p. (B) Fingerprint region of the TOCSY spectrum of E1p truncated using endoproteinase GluC.

exchange cross-peaks "linking" folded and unfolded species that are in equilibrium have been observed for folding intermediates of bovine pancreatic trypsin inhibitor (BPTI) (*48*, *49*). On the basis of estimates of the likely T_1 values for Nterm-E1p, we suggest that the rate of exchange between the folded and unfolded Nterm-E1p molecules at 298 K is in the range of 0.5−5 s^{-1}.

The TOCSY experiment was repeated at 284 K, which yielded the same folded:unfolded ratio for the Nterm-E1p species as was found at 298 K. However, now no exchange cross-peaks between the folded and unfolded tryptophan NH resonance are observed. Additionally, no exchange cross-peaks in the low-field region of the TOCSY spectrum are observed under these conditions. Thus, temperature does seriously affect the exchange rate, but it does not affect the folding equilibrium of the Nterm-E1p species.

NMR Characterization of the 200 kDa E1p Homodimer

The observed dynamic exchange between the folded and unfolded state of Nterm-E1p suggests that the N-terminal domain of E1p is highly mobile. In the past, flexibility of regions of E1p was suggested on basis of the sensitivity of E1p to proteases (*22*) and on the basis of its resistance to crystallization (W. Hol, personal communication). Highly mobile parts of a protein should be visible in an NMR experiment, even if the entire protein is very large (the E1p dimer has a molecular mass of 2 × 100 kDa). For this reason, 1D ^{1}H (data not shown) and 2D ^{1}H TOCSY (Figure 7A) NMR spectra of the intact E1p at pH 5.5 were recorded. The 1D and 2D NMR spectra exhibit a number of sharp resonances normally not expected for a structured enzyme with the size of E1p. ThDP (E1p's cofactor) was present in the sample in very small excess. The resonances originating from free ThDP were identified, and clearly, besides these resonances, the spectra contain additional sharp resonances (Figure 7A), indeed confirming the presence of highly mobile regions in E1p. Most of these resonances are found in the 7.8−8.6 ppm region, suggesting unstructured parts of the protein. Upon comparison of the E1p NMR spectra with the NMR spectra of Nterm-E1p, we were unable to identify distinct cross-peak patterns at comparable chemical shifts in both spectra. Nevertheless, the TOCSY spectrum of E1p shows some similarity to the spectrum of the unfolded peptide. Thus, although the entire E1p contains highly flexible regions, we are, on the basis of these experiments, unable to unambiguously prove that these peaks originate from residues in its N-terminal domain.

To determine whether the observed sharp resonances originate from the N-terminal region of E1p, or from other flexible regions in the enzyme, the sample was partially digested with endoproteinase GluC. This protease cuts E1p at amino acid residue E40, and thus, digestion results in removal of amino acid residues 1−40. The subsequently recorded 2D ^{1}H TOCSY NMR spectrum is shown in Figure 7B. Comparison of the spectra of digested and undigested E1p shows that quite a number of sharp resonances in the spectrum of the complete E1p have disappeared in the spectrum of the truncated E1p. Thus, it seems that at least some of the sharp resonances originate from N-terminal residues 1−40 of E1p. Some sharp resonances, however, are not affected by truncating E1p, suggesting that these resonances originate either from another mobile region of E1p or from impurities in the sample that are not sensitive to the protease. Previously, we demonstrated that the core of E1p starts at amino acid 49; therefore, truncation at amino acid 40 likely results in a small N-terminal "tail". This could explain why the 2D ^{1}H TOCSY spectrum of the truncated E1p still contains sharp resonances. Moreover, E1p is cleaved by chymotrypsin and trypsin at residue R418 and residue R554, respectively (*22*). It seems likely that exposed loops or turns are present at these sites. Possibly, these loops are flexible, causing sharp NMR resonances. Nevertheless, these results strongly indicate that the N-terminal region of E1p is flexible, analogous to Nterm-E1p.

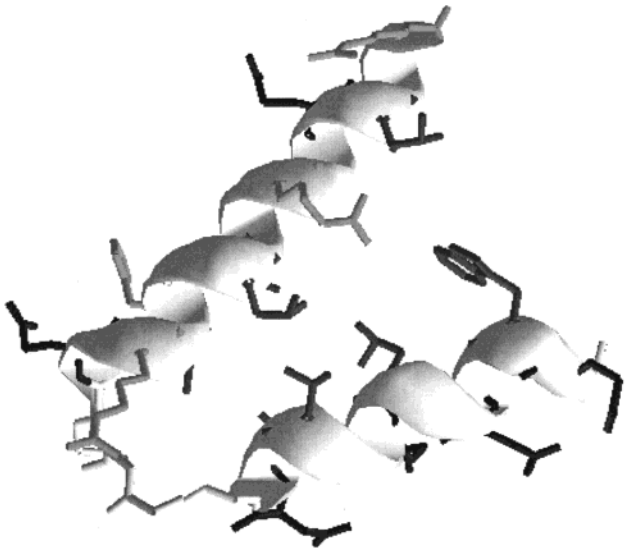

FIGURE 8: Model of the N-terminal domain of E1p as inferred from a secondary structure prediction and our NMR, CD, and fluorescence spectroscopy data. For a description of the model, the reader is referred to the Discussion.

DISCUSSION

In the study presented here, the structural and functional characterization of a synthetic peptide (Nterm-E1p) that represents the N-terminal region of E1p is described.

Previous experiments showed that the N-terminal region of E1p is necessary for the binding of E1p to E2p (*23*).

Using activity and binding assays, it is demonstrated that the peptide Nterm-E1p binds to E2p and that in doing so specifically competes with E1p. Furthermore, the peptide has no influence on the binding of E3 to E2p. Thus, here it is unambiguously proven that the N-terminal region of E1p forms a separate domain involved in the binding to E2p. Moreover, these experiments justify the use of the synthetic peptide for the characterization of the structure and function of the N-terminal domain of E1p.

Both the CD experiment (Table 1) and the 2D NMR analysis of Nterm-E1p at pH 4.8 indicate that the peptide has a high α-helical content. The calculated secondary structure content of Nterm-E1p at pH 4.8 based on the CD data is remarkably similar to the predicted secondary structure content of the peptide based on an analysis by the neural network algorithms from the European Molecular Biology Laboratory (EMBL) (*50*, *51*). From the secondary structure prediction and our own data, the following model of the N-terminal domain of E1p is inferred (Figure 8). The domain likely consists of two α-helices connected by a loop or turn. Because residues 1−8 could be removed without affecting E1p, these residues probably do not belong to the first helix. Since the E1p "core" starts at amino acid 49 and residues R37, E40, and R44 are highly sensitive to proteases, it seems very likely that this region forms an extended linker, connecting the N-terminal domain to the E1p core. Analysis of the sequences of the putative α-helices in the N-terminal domain shows that mainly the first helix (approximately amino acids 13−25) has a high content of acidic residues. A helical wheel of this sequence shows that D17, E20, and D24 are all on the same side of the amphipatic helix, separated by a single turn. The opposite side of the helix has the same pattern, but now with hydrophobic residues. The second helix (for which it is less evident where is starts and ends) also has one side that has a high content of hydrophobic residues. We suggest therefore that the N-terminal domain is formed by these two helices, the hydrophobic patches of which interact, forming a hydrophobic core. The acidic residues of helix 1 form the region of binding to E2p. Mutagenesis experiments are in progress to prove this hypothesis.

Using CD, fluorescence, and NMR spectroscopy, it is demonstrated that the peptide is present in two conformations, the population of which depends on the sample conditions. The conformations are designated unfolded at pH >6, where the peptide is largely unfolded, and folded at pH <5, where a mixture of the folded and unfolded peptide exists.

The equilibrium between the folded and unfolded state of the peptide is affected not only by the pH but also by the ionic strength as NMR spectra show. The rate of exchange between the folded and unfolded Nterm-E1p molecules is suggested to be in the range of $0.5-5\ s^{-1}$. Similar exchange rates were found for the exchange between the folded and unfolded state of the BPTI folding intermediates (*48*, *49*). Just as in the case of the BPTI folding intermediates, the folded conformation of Nterm-E1p is not very stable.

As mutagenesis experiments identified basic residues in the E1/E3 binding domain and catalytic domain as the binding residues for E1p (*18*), it is likely that the acidic residues in the N-terminal domain are involved in ionic interactions between E1p and E2p. Shielding of these charges might mimic the bound state of the N-terminal domain, resulting in a shift in the equilibrium toward the folded state.

It is surprising that at pH >6 the peptide is unfolded as at this pH E1p binds very well to E2p. However, it is possible that interaction with E2p induces a folded conformation (analogous to the charge shielding effect). Alternatively, removal of the folded N-terminal domain by binding to E2p will force the equilibrium in the folded direction, since the folded and unfolded conformations are in slow exchange. Finally, the possibility that interactions of the N-terminal domain of E1p with the E1p core stabilize the folded conformation of the N-terminal domain cannot be excluded.

Sharp resonances in the NMR spectra of the complete E1p (Figure 7) unambiguously demonstrate that the 200 kDa enzyme contains highly flexible regions. Because several of these resonances are absent in the spectrum of the truncated E1p, it is very likely that the N-terminal region of E1p (amino acid 1−48) is flexible in the native enzyme. Efficient binding of E1p to E2p requires residues on both the binding and catalytic domain of E2p (*18*). Only an E1p dimer (containing two N-terminal domains) and not a monomer or heterodimer (containing one N-terminal domain) binds strongly to E2p (*23*). The requirement for two N-terminal domains is most likely due to the distance between the binding residue R416 on the catalytic domain of E2p and the C-terminal helix of the binding domain of E2p, which is too large to be spanned by one N-terminal domain of E1p. Since E1p interacts with two different binding sites on E2p, it is likely that the flexible regions are necessary for the enzyme to be able to adapt to the two required "binding conformations". The observed dynamic character of Nterm-E1p is possibly required for its binding to E2p. After the first N-terminal domain of the E1p dimer binds to E2p, a high degree of flexibility of E1p will

be required to interact with the second binding site on E2p. Recent 3D electron microscopy of *Saccharomyces cerevisiae* E2p (*52*) revealed striking dynamics of the E2p core; a 40 Å difference in diameter was observed. Moreover, the intact complex exhibits flexibility similar to that of the E2p core, and the E1p on the outside of the core mimics the movements of the underlying E2p core. It is therefore quite likely that the flexible regions observed in E1p and Nterm-E1p are involved in this dynamic process, assuming that this core flexibility is also present in the cubic E2p cores.

Finally, the flexibility of E1p, and possibly the flexibility of the N-terminal domain of E1p, can also be important for the catalytic properties of the enzyme. E1p is an allosteric enzyme, therefore requiring conformational freedom of the active site of the enzyme in the multienzyme complex.

In summary, E1p has an independent N-terminal folding domain that is necessary for binding of E1p to E2p. The domain (in the isolated peptide) samples both a folded and an unfolded conformation, the population of which is determined by pH and ionic strength. The observed exchange between the two conformations of the N-terminal domain and the flexible regions that we identified in the entire E1p are very likely necessary for the binding of E1p to E2p.

ACKNOWLEDGMENT

We thank Arie van Hoek for his contribution to the time-resolved fluorescence measurements and Sjef Boeren for his contribution to the MALDI measurement.

REFERENCES

1. Perham, R. N. (1991) *Biochemistry 30*, 8501−8512.
2. Mattevi, A., De Kok, A., and Perham, R. N. (1992) *Curr. Opin. Struct. Biol. 2*, 877−887.
3. Berg, A., and De Kok, A. (1997) *Biol. Chem. Hoppe-Seyler 378*, 617−634.
4. De Kok, A., Hengeveld, A. F., Martin, A., and Westphal, A. H. (1998) *Biochim. Biophys. Acta 1385*, 353−366.
5. Perham, R. N. (2000) *Annu. Rev. Biochem. 69*, 961−1004.
6. Mattevi, A., Obmolova, G., Schulze, E., Kalk, K. H., Westphal, A. H., De Kok, A., and Hol, W. G. J. (1992) *Science 255*, 1544−1550.
7. Mattevi, A., Obmolova, G., Kalk, K. H., Westphal, A. H., De Kok, A., and Hol, W. G. J. (1993) *J. Mol. Biol. 230*, 1183−1199.
8. Knapp, J. E., Mitchell, D. T., Yazdi, M. A., Ernst, S. R., Reed, L. J., and Hackert, M. L. (1998) *J. Mol. Biol. 280*, 655−668.
9. Knapp, J. E., Carroll, D., Lawson, J. E., Ernst, S. R., Reed, L. J., and Hackert, M. L. (2000) *Protein Sci. 9*, 37−48.
10. Izard, T., ×ae×ae×aeÆvarsson, A., Allen, M. D., Westphal, A. H., Perham, R. N., de Kok, A., and Hol, W. G. J. (1999) *Proc. Natl. Acad. Sci. U.S.A. 96*, 1240−1245.
11. Dardel, F., Davis, A. L., Laue, E. D., and Perham, R. N. (1993) *J. Mol. Biol. 229*, 1037−1048.
12. Green, J. D., Laue, E. D., Perham, R. N., Ali, S. T., and Guest, J. R. (1995) *J. Mol. Biol. 248*, 328−343.
13. Ricaud, P. M., Howard, M. J., Roberts, E. L., Broadhurst, R. W., and Perham, R. N. (1996) *J. Mol. Biol. 264*, 179−190.
14. Berg, A., Vervoort, J., and De Kok, A. (1996) *J. Mol. Biol. 261*, 432−442.
15. Berg, A., Vervoort, J., and De Kok, A. (1997) *Eur. J. Biochem. 244*, 352−360.
16. Kalia, Y. N., Brocklehurst, S. M., Hipps, D. S., Appella, E., Sakaguchi, K., and Perham, R. N. (1993) *J. Mol. Biol. 230*, 323−341.
17. Mande, S. S., Sarfaty, S., Allen, M. D., Perham, R. N., and Hol, W. G. J. (1996) *Structure 4*, 277−286.
18. Schulze, E., Westphal, A. H., Boumans, H., and De Kok, A. (1991) *Eur. J. Biochem. 202*, 841−848.
19. Schulze, E., Westphal, A. H., Veeger, C., and de Kok, A. (1992) *Eur. J. Biochem. 206*, 427−435.
20. Ævarsson, A., Seger, K., Turley, S., Sokatch, J. R., and Hol, W. G. J. (1999) *Nat. Struct. Biol. 6*, 785−792.
21. Ævarsson, A., Chuang, J. L., Wynn, R. M., Turley, S., Chuang, D. T., and Hol, W. G. J. (2000) *Struct. Folding Des. 8*, 277−291.
22. Hengeveld, A. F., Westphal, A. H., and De Kok, A. (1997) *Eur. J. Biochem. 250*, 260−268.
23. Hengeveld, A. F., Schoustra, S. E., Westphal, A. H., and de Kok, A. (1999) *Eur. J. Biochem. 265*, 1098−1107.
24. Gibson, T. J. (1984) Ph.D. Thesis, University of Cambridge, Cambridge, U.K.
25. Hanemaaijer, R., Westphal, A. H., Berg, A., Van Dongen, W., De Kok, A., and Veeger, C. (1989) *Eur. J. Biochem. 181*, 47−53.
26. Westphal, A. H., and De Kok, A. (1988) *Eur. J. Biochem. 172*, 299−305.
27. Benen, J., van Berkel, W., Veeger, C., and de Kok, A. (1992) *Eur. J. Biochem. 207*, 499−505.
28. Khailova, L. S., Bernhardt, R., and Huebner, G. (1977) *Biokhimya 42*, 113−117.
29. Bresters, T. W., de Abreu, R. A., de Kok, A., Visser, J., and Veeger, C. (1977) *Eur. J. Biochem. 59*, 335−345.
30. Benen, J., van Berkel, W., Zak, Z., Visser, T., Veeger, C., and De Kok, A. (1991) *Eur. J. Biochem. 202*, 863−872.
31. Schwartz, E. R., and Reed, L. J. (1970) *Biochemistry 9*, 1434−1439.
32. Schägger, H., and Von Jagow, G. (1987) *Anal. Biochem. 166*, 368−379.
33. Goa, J. (1953) *Scand. J. Clin. Lab. Invest. 5*, 218−222.
34. Kraehenbuhl, J. P., Galardy, R. E., and Jamieson, J. D. (1974) *J. Exp. Med. 139*, 208−223.
35. Novikov, E. G., van Hoek, A., Visser, A. J. W. G., and Hofstraat, J. W. (1999) *Opt. Commun. 166*, 189−198.
36. Kumar, A., Ernst, R. R., and Wüthrich, K. (1980) *Biochem. Biophys. Res. Commun. 95*, 1−6.
37. Macura, S., and Ernst, R. R. (1980) *Mol. Phys. 41*, 95−117.
38. Braunschweiler, L., and Ernst, R. R. (1983) *J. Magn. Reson. 53*, 521−528.
39. Bax, A., and Davis, D. G. (1985) *J. Magn. Reson. 65*, 355−360.
40. Griesinger, C., Otting, G., Wüthrich, K., and Ernst, R. R. (1988) *J. Am. Chem. Soc. 110*, 7870.
41. Marion, D., and Wüthrich, K. (1983) *Biochem. Biophys. Res. Commun. 113*, 967−974.
42. Bosma, H. J., De Kok, A., Westphal, A. H., and Veeger, C. (1984) *Eur. J. Biochem. 142*, 541−549.
43. Provencher, S. W., and Glockner, J. (1981) *Biochemistry 20*, 33−37.
44. Lakowicz, J. R. (1999) in *Principles of fluorescence spectroscopy*, 2nd ed., Kluwer Academic/Plenum Publishers, New York.
45. Chen, Y., and Barkley, M. D. (1998) *Biochemistry 37*, 9976−9982.
46. Visser, A. J. W. G., and Lee, J. (1980) *Biochemistry 19*, 4366−4372.
47. Bundi, A., and Wüthrich, K. (1979) *Biopolymers 18*, 285−298.
48. van Mierlo, C. P. M., Darby, N. J., Neuhaus, D., and Creighton, T. E. (1991) *J. Mol. Biol. 222*, 373−390.
49. van Mierlo, C. P. M., Darby, N. J., Keeler, J., Neuhaus, D., and Creighton, T. E. (1993) *J. Mol. Biol. 229*, 1125−1146.
50. Rost, B., and Sander, C. (1993) *J. Mol. Biol. 232*, 584−599.
51. Rost, B., and Sander, C. (1994) *Proteins 19*, 55−72.
52. Zhou, Z. H., Liao, W., Cheng, R. H., Lawson, J. E., McCarthy, D. B., Reed, L. J., and Stoops, J. K. (2001) *J. Biol. Chem. 276*, 21704−21713.

BI012172U